Proceedings World Geothermal Congress 2026
Calgary, Canada, June 8 – 11, 2026

Optimisation of ATES in Conjunction With E-Grid in Integrated Heating Systems

Amirhossein Hashemi[1]*, Martin Bloemendal[1,2], Philip J Vardon[1]
[1]Delft University of Technology, Faculty of Civil Engineering and Geosciences, Delft, Netherlands
[2]TNO, Dutch Geological Survey, Utrecht, Netherlands
*a.hashemi-2@tudelft.nl

Keywords: Aquifer Thermal Energy Storage (ATES), Thermal Regeneration, Grid Flexibility, Demand Shifting, Free Cooling

ABSTRACT

Aquifer Thermal Energy Storage (ATES) provides a key opportunity to integrate electrified heating and cooling with the E-grid by shifting thermal loads and stabilising E-grid demand. This study evaluates two ATES systems at TU Delft, ECHO and NEXT, to investigate how control, regeneration, and system integration influence operational efficiency and thermal balance under real operating conditions. NEXT, an all-electric office building, is connected to the campus thermal ring, which supplies NEXT and another building from a shared ATES system (two warm and two cold wells), while the above-ground installation serves NEXT only. ECHO has a stand-alone ATES (one warm and one cold well) system designed for low-temperature supply. Multi-year monitoring data are analysed using indicators including coefficient of performance (COP), compressor runtime, and energy balance. Both systems achieved high passive-cooling shares (i.e., over 80%) and stable heating COPs of 4-5, confirming efficient performance. NEXT maintained near-symmetric seasonal balance through frequent regeneration supported by the thermal ring, whereas ECHO progressively improved toward balance through late-summer recovery of energy balance. The findings demonstrate that well-controlled ATES operation can enhance flexibility, sustain storage efficiency, and enable grid-compatible electrified heating and cooling within integrated energy systems.

1 INTRODUCTION

Electrification of heating and cooling is widely recognised as a key pathway towards decarbonising the building sector, while simultaneously introducing challenges for the electricity grid (E-grid) in terms of stability and flexibility (IRENA, 2020, Hewitt, 2024). In many regions, the coincidence of winter heating and summer cooling demands with peak electricity use is associated with network congestion and capacity constraints. Without flexible thermal storage or demand-side response, large-scale electrification is expected to intensify peak loads (Bloemendal et al., 2014, Li et al., 2023).

Thermal energy storage and demand-side flexibility have therefore been identified as key enablers for aligning electrified demand with grid constraints and renewable-dominated supply. Shifting electric heating and/or cooling to periods of abundant renewable generation, and storing thermal energy to decouple the timing of supply and demand, are recognised as effective measures to mitigate supply variability and rising electricity demand (Bloemendal et al., 2018, Buonocore et al., 2022).

In this regard, Aquifer Thermal Energy Storage (ATES) has been identified as a scalable option for reducing the mismatch between thermal and electrical demand in integrated heating and cooling systems (Beernink et al., 2022). By seasonally storing heat and cold in groundwater aquifers, loads can be shifted and grid stress alleviated (Fleuchaus et al., 2018). When combined with heat pumps and responsive controls, ATES has been shown to support grid-compatible operation through adjustments in operating modes to reflect electricity availability, renewable-generation patterns, or system constraints (Lee, 2010, Lund et al., 2014, Buffa et al., 2019).

The performance of electrified heating and cooling systems is strongly shaped by the magnitude and temporal variability of building heating and cooling loads. These load fluctuations influence instantaneous COP, heat-pump electricity use, passive-cooling availability, and the frequency or intensity of regeneration cycles, all of which determine the interaction between thermal systems and the electricity grid (Finck et al., 2018, Nuytten et al., 2013). Previous studies have shown that ATES systems exhibit performance that depends not only on aquifer conditions and control strategies but also on how real, dynamic thermal demands are met throughout the year (Fleuchaus et al., 2018, Beernink et al., 2022). Consequently, assessing monitored performance under varying

load conditions is essential for understanding how ATES systems operate in practice, how efficiently thermal demands are met, and how these systems contribute to grid-compatible electrified heating and cooling.

In this study, 2 ATES systems at TU Delft are evaluated to quantify the operational energy performance of electrified heating and cooling relevant for their grid-compatibility. Using monitored datasets, performance indicators including the coefficient of performance (COP), seasonal energy balance, passive-cooling share, compressor runtime fraction, energy balance regeneration, storage temperature, and operating-mode distributions are examined. The analysis links monitored storage dynamics, operational mode occurrence distributions, and control responses of the 2 ATES systems to seasonal efficiency and patterns consistent with grid-flexible energy operation.

2 SYSTEMS AND DATA

Two ATES-equipped buildings on the TU Delft campus, NEXT and ECHO, are examined as representative installations operating under distinct supervisory controls and data resolutions. Both employ ATES for seasonal heating and cooling but differ in network integration, mode complexity, and measurement granularity. In both systems, heating is supplied by heat pumps that extract heat from the warm well and upgrade it to meet building demand, while cooling is provided either passively through direct groundwater circulation or actively via heat pump operation when required. Passive cooling occurs when groundwater temperatures are sufficiently low to satisfy cooling demand without compressor use, significantly reducing electricity consumption. While both systems rely on the same underlying ATES principles, they differ in how thermal energy is distributed and managed at the system level, which influences their operational flexibility and interaction with the electricity grid.

NEXT is connected to the campus thermal ring, which provides the hydraulic connection to the shared underground ATES, while the above-ground installation operates solely for NEXT. Twelve operating modes (Table 1) were defined for NEXT (N), covering heating (H), cooling (C), regeneration (R), and combined (B) operation, each characterised by specific ATES charging or discharging pathways. Although the thermal ring provides a shared subsurface system, the operating modes analysed here represent NEXT's own building-level operation. Daily subsystem records were available, including groundwater extraction and injection temperatures, supply and return temperatures to the ring and the building, and electricity use of heat pumps and circulation pumps. The mode classification was used to reconstruct control actions, energy-exchange pathways, and operational efficiency under varying temperature and load conditions.

Table 1. Operational modes and energy flows: NEXT

Mode	Function (purpose + delivered energy)	ATES Interaction
N: H1	Heating via HP	HW discharged; return to CW
N: R1	CW regeneration via DC	HW discharged; CW charged via DC
N: H2	Heating via HP + CW regeneration	HW discharged; CW charged via DC
N: H3	Heating via HP + DC cooling (series)	HW discharged; CW charged via DC (series)
N: H4	Heating via HP + DC cooling (parallel)	HW discharged; CW charged via DC (parallel)
N: R2	HW regeneration via DC	CW discharged; HW charged via DC
N: C1	Passive cooling + HW regeneration	CW discharged; HW charged via DC
N: B1	Cooling via HP > heating via HP	CW discharged; return to HW
N: C2	Cooling via HP	No ATES use
N: C3	Cooling via HP + HW regeneration	CW discharged; HW charged via HP condenser
N: C4	Cooling via HP (Reject to DC)	CW discharged; no HW charge
N: C5	Cooling via HP + HW regeneration	CW discharged; HW charged via HP condenser (direct)

* HW: warm well; CW: cold well; HP: heat pump; DC: dry cooler

ECHO is an educational building with a stand-alone ATES doublet supported by two electric heat pumps and 1,200 rooftop PV panels. Operational modes are structured into detailed heating (H), cooling (C), and combined (B) operation (Table 2) for ECHO, with the prefix 'E:' indicating ECHO modes, and with sub-modes distinguishing passive cooling, HP-driven cooling, DC-assisted cooling, combined heating–cooling states, and ATES or non-ATES operation. Daily subsystem records were available, including electricity use of the heat pumps and circulation pumps, and well temperatures. On the ATES side, only monthly values were available for delivered

thermal energy and groundwater extraction and injection temperatures. Despite these differing resolutions, the classification enables clear identification of transitions between heating and cooling seasons and supports the assessment of seasonal energy balance and performance trends.

Table 2. Operational modes and energy flows: ECHO

Mode	Function (purpose + delivered energy)	ATES Interaction
E: H1	Heating via HP + limited buffer cooling	HW discharged; return to CW
E: H1.1	Heating via HP + DC cooling (*0–5 °C)	HW discharged; CW charged via DC (series)
E: H1.2	Heating via HP + DC cooling (*−5–0 °C)	HW discharged; CW charged via DC (parallel)
E: H1.3	Heating via HP + DC cooling (*5–10 °C)	HW discharged; CW charged via DC (parallel)
E: C1	Cooling via DC + CW regeneration (*≥ 0 °C)	HW discharged; CW charged via DC
E: B1	Cooling via HP > heating via HP	CW discharged; return to HW
E: C2	Passive cooling	CW discharged; return to HW
E: C3	Passive cooling + HW regeneration	CW discharged; HW charged via DC
E: C4	Cooling via HP + HW regeneration	CW discharged; HW charged via HP condenser
E: C5	Cooling via HP (Reject to DC)	CW discharged; no HW charge
E: C6	(No ATES) Cooling via HP	No ATES use
E: B2	(No ATES) Heating via boiler + Cooling via DC	No ATES use

* Outdoor temperature in parentheses.

Table 1 and Table 2 summarise the operational logic by linking each mode to its associated heating or cooling function, ATES interaction (charging or discharging of cold well (CW) or hot well (HW)), and the specific pathway, direct circulation, charging via dry-cooler, or condenser-side heat rejection, through which thermal exchange occurs. This mapping forms the basis for grid-relevant indicators used in the analysis, including passive-cooling share, compressor-runtime fraction, regeneration frequency, and seasonal thermal balance (Nuytten et al., 2013, Finck et al., 2018, Fleuchaus et al., 2018).

3 METHODOLOGY

3.1 Analytical framework

This study evaluates ATES operation across a three-year period (2022–2024) with respect to E-grid compatibility by constructing operating-mode timelines from measured data and process and instrumentation diagrams (P&IDs) for both buildings. Control states recorded in the Building Management Systems (BMS) logs are mapped to mode labels consistent with the P&ID-defined hydraulics and equipment states, ensuring comparable interpretation despite differing data resolutions (daily for NEXT; monthly on the ATES side and daily on the building side for ECHO). Each day was assigned to a single operating mode; regeneration intervals are identified from dry-cooler operation or heat-pump condenser heat rejection as specified in the P&IDs. The resulting timelines are used to organise the computation and comparison of the performance indicators defined in Section 3.2, which capture grid-relevant behaviour (e.g., passive operation share, compressor use, and charging activity).

3.2 Performance indicators

The daily COP expresses the daily efficiency of the system, defined as the ratio of daily thermal energy delivered to the building ($Q_{delivered}$, MWh) to the total daily electrical energy consumed ($E_{electric}$, MWh) by compressors and circulation pumps:

$$COP = {Q_{delivered}}/{E_{electric}} \quad (1)$$

Higher COP values indicate more heat or cooling delivered per unit of electricity, implying reduced stress on the E-grid during operation. The $Energy\ Balance$ (B) describes the net energy symmetry of the storage medium and indicates whether the system predominantly operates in heating or cooling mode:

$$Energy\ Balance\ (\%) = 100 * \frac{E_{inj}(Cold) - E_{inj}(Warm)}{E_{inj}(Cold) + E_{inj}(Warm)} \quad (2)$$

where $E_{inj}(Cold)$ is energy injected into the cold well over the season and $E_{inj}(Warm)$ is energy injected into the warm well over the season. A value close to zero signifies balanced operation, whereas positive or negative values denote heating- or cooling-dominant behaviour. A balanced ATES is essential for long-term aquifer sustainability and stable thermal recovery. The passive-cooling share ($C_{passive}$) was computed as the ratio of the daily thermal energy extracted from the ATES to the total daily thermal energy delivered to the building:

$$C_{passive}\ (\%) = 100 * \frac{Q_{cold}(passive)}{Q_{cold}(total)} \quad (3)$$

where $Q_{cold}(passive)$ is the cooling energy provided through direct groundwater circulation, and $Q_{cold}(total)$ is the total cooling energy demand. Higher $C_{passive}$ values signify stronger utilisation of natural thermal gradients, reducing electrical consumption during high-load hours. The heat pump compressor runtime fraction ($F_{compr\ runtime}$) was approximated from daily energy records as the ratio between the electricity consumed by the heat pump compressor and the total system electricity use:

$$F_{compr\ runtime}(\%) = 100 * \frac{W_{HP,day}}{W_{total,day}} \quad (4)$$

where $W_{HP,day}$ denotes the daily electricity use of the heat-pump compressor, and $W_{total,day}$ (MWh) represents the total daily electrical consumption of the thermal system (compressor + circulation pumps + auxiliary devices). Lower RF values suggest longer periods of passive operation or improved alignment with off-peak electricity periods. Finally, the regeneration frequency (R_{freq}) reflects how often the system switches into regeneration or charging modes during a season:

$$R_{reg} = N_{trans,reg} \quad (5)$$

where $N_{trans,reg}$ is the number of days associated with regeneration or charging modes (e.g., via dry-cooler or condenser-side charging). Frequent regeneration events imply proactive utilisation of renewable thermal energy or low-price electricity periods for storage pre-charging, a key aspect of grid-compatible operation. In addition, well temperatures were monitored to assess how well temperatures, at the thermal ring (NEXT) or aquifer (ECHO), influence overall efficiency. Variations in these temperatures directly affect achievable COP values and determine whether the system operates within favourable temperature ranges for passive or compressor-driven modes.

3.3 Data treatment and comparison

All datasets were checked for sensor gaps and inconsistencies, then aggregated to a daily timeline aligned with the operating-mode labels. NEXT data were used at their native daily resolution. For ECHO, monthly ATES totals were evenly distributed across the days of each month to create daily series, which were subsequently combined with the building-side daily measurements.

4 RESULTS

4.1 NEXT PERFORMANCE

4.1.1 Operational Modes and Seasonal Distribution

Figure 1 presents the monthly distribution of NEXT's operating modes. The daily records show that several modes often coexist within a single month. In July 2024, mixed operation dominated, but regeneration and cooling-only modes also occurred, whereas in January 2024, operation was primarily heating-oriented with short regeneration cycles targeting the cold well. Across 2022–2024, the system gradually evolved toward smoother alternation between heating and cooling, suggesting improved coordination between storage use and seasonal demand. While the daily resolution captures these recurring transitions, the absence of sub-daily data limits observation of individual control responses or rapid load adjustments.

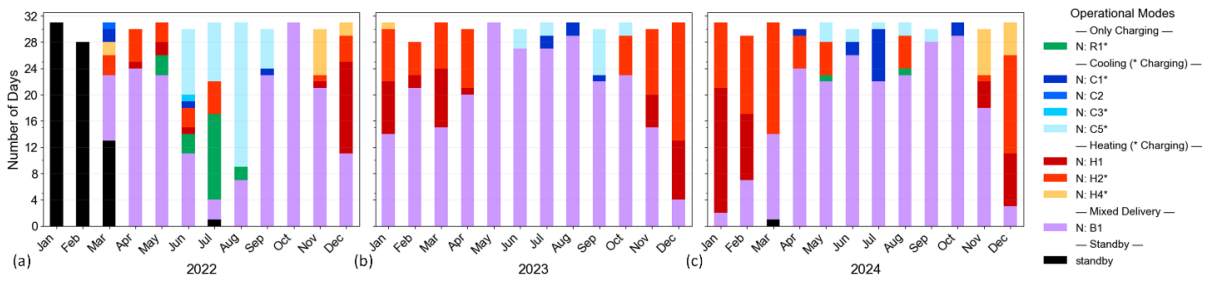


Figure 1. NEXT operating modes by month: number of days in each mode: (a) 2022, (b) 2023, (c) 2024.

4.1.2 Electricity Demand and Outdoor Temperature

The relationship between total electricity consumption and outdoor temperature illustrates the contrasting behaviour of cooling and heating operation (Figure 2). In summer months, when cooling demand was high, total daily electricity use remained below 0.1 MWh (mostly for circulation), reflecting predominantly passive cooling. In winter, heating demand reached up to 7 MWh/day, with electricity consumption often exceeding 1.2 MWh/day as compressors operated continuously to meet heating demands. The narrow spread of daily electricity values under similar outdoor temperature conditions demonstrates stable, consistent operation, with no abrupt peaks observed throughout 2022–2024. A small number of irregular points appear in Figure 2. On a few cooling days, electricity use is higher than expected for the corresponding outdoor temperatures due to temporarily reduced passive-cooling performance, during which the heat pump provided part of the cooling demand. Conversely, several winter days show unrealistically low or near-zero heat-pump electricity despite normal heating output; these points reflect brief metering dropouts rather than actual operational behaviour.

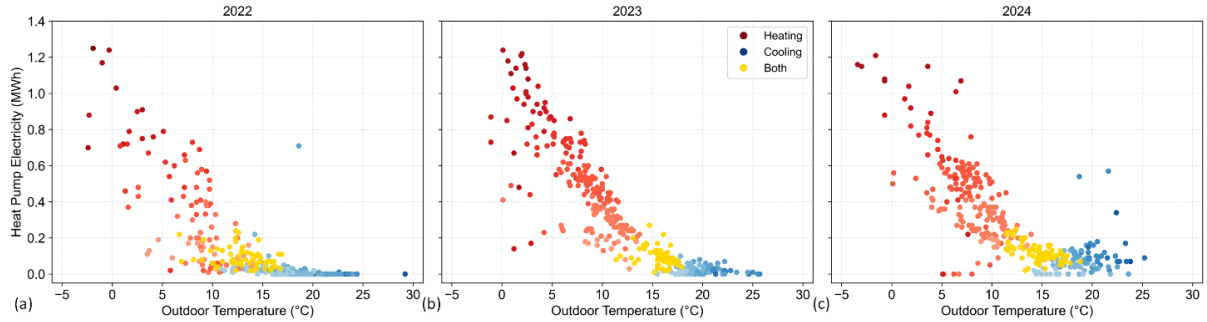


Figure 2. NEXT daily electricity consumption vs. outdoor temperature: (a) 2022, (b) 2023, (c) 2024; colour intensity indicates daily delivered thermal energy (0–7 MWh).

4.1.3 Passive Cooling and Compressor Operation

As shown in Figure 3, total cooling energy is high from June to September, with a peak of ≈80 MWh in July 2024, while compressor runtime generally remains below 60% during the cooling period. The strong inverse correlation between compressor use (F) and delivered cold energy (Cold) (F–Cold = –0.95 to –0.84 across 2022–2024) further confirms that higher cooling loads are predominantly met through passive ATES operation rather than mechanical cooling. The passive-cooling share (C) stays high, typically over 80%, confirming that most cooling is supplied directly through groundwater circulation with limited compressor input. This results in low electrical demand during the cooling season, minimising the system's contribution to grid load when ambient temperatures are high. In August 2022 a total of 59.9 MWh of cooling was delivered with 2.4 MWh of electricity and near-zero heat pump runtime. If the same cooling load had been produced mechanically by a chiller or heat pump with a COP of 4, the required electricity would have been approximately 15.0 MWh, about 12.6 MWh (≈ 84%) higher than observed. This example highlights the significant reduction in electrical demand achieved through passive ATES cooling, underscoring its role in alleviating grid load during high-temperature periods.

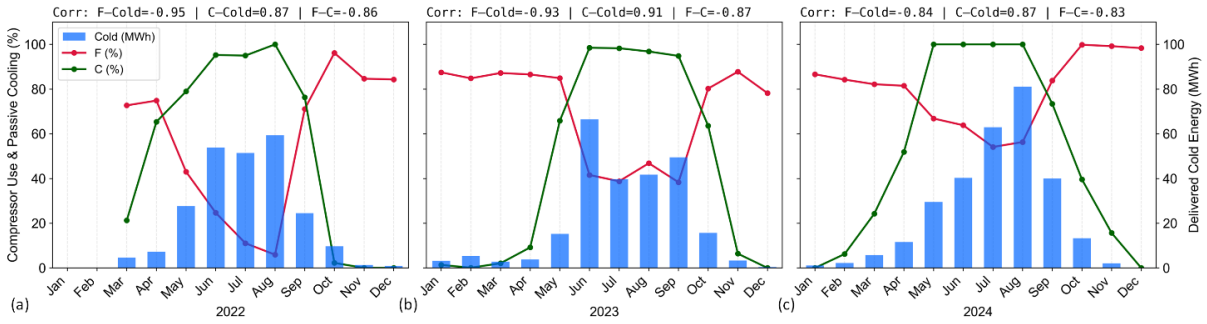


Figure 3. NEXT monthly cold energy (Cold), passive-cooling share (C), and compressor runtime fraction (F) (a–c).

During winter, when cooling demand is minimal, compressor runtime increases sharply as the heat pumps operate continuously for space heating. In January 2024, runtime approached ≈85% (near full load), and daily electricity use exceeded ≈ 1.2 MWh, with outdoor temperature of -5 °C. The heating period therefore remains electricity-intensive; however, the operation is steady and well-controlled, with no evidence of short-term power fluctuations. Despite higher electrical input, the system operates with supply temperatures below 45 °C, allowing the heat pumps to maintain acceptable COP values of 4–5 (Figure 4), consistent with efficient heating. This performance is supported by a stable temperature from the thermal ring (i.e., HEX entry temperature ≈ 15 °C). Together, these patterns show that while summer cooling reduces grid stress through passive cooling, winter heating sustains high efficiency, ensuring reliable comfort with predictable electrical demand.

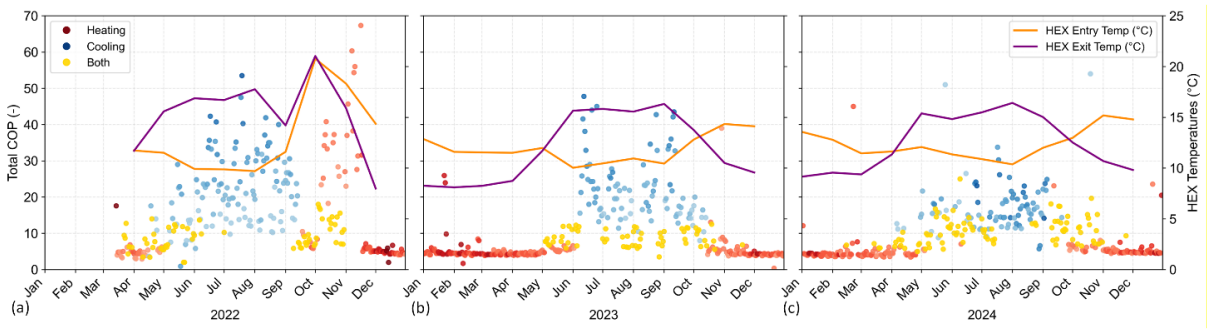


Figure 4. NEXT daily COP and thermal-ring (entry and exit) temperature: (a) 2022, (b) 2023, (c) 2024.

4.1.4 Energy Balance and Regeneration Frequency

Figure 5 shows that NEXT maintains a nearly symmetric energy balance throughout 2022–2024. In early 2022, the system displayed a slightly cooling-dominant trend, which diminished over time as regeneration became more evenly distributed. By 2024, the monthly balance remained within ±15%, reflecting improved alignment between thermal extraction and injection and an overall trend toward balance. Regeneration occurs on multiple days per month, using condenser heat in winter and dry-cooler operation in summer. These events stabilise subsurface temperatures and prevent long-term drift, sustaining the storage capacity of the aquifer. Maintaining this equilibrium ensures consistent thermal performance from year to year and enables the system to act as a stable thermal buffer that supports continuous electrified heating and cooling.

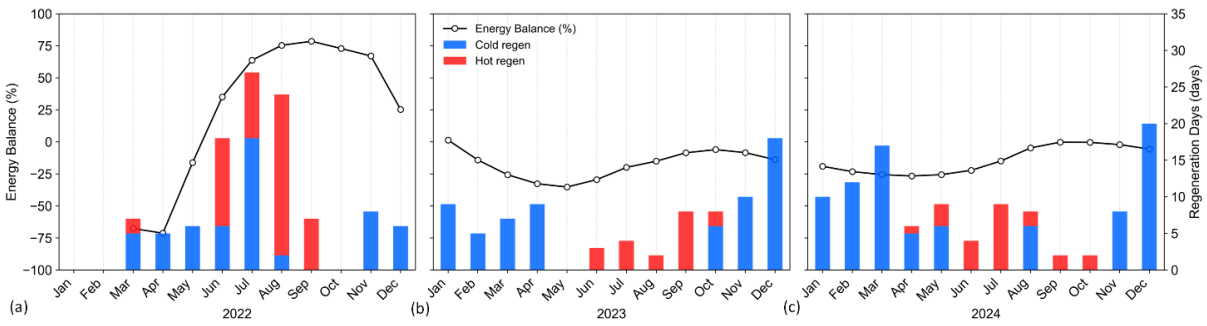


Figure 5. NEXT monthly ATES energy balance and regeneration days (a–c); regeneration includes condenser and dry-cooler charging.

4.2 ECHO BUILDING PERFORMANCE

4.2.1 Operational Modes and Seasonal Distribution

Figure 6 shows the monthly distribution of ECHO's operating modes. The building alternates clearly between cooling-dominant operation in summer and heating-dominant operation in winter, with only brief mixed periods during transitional months. In July 2023, operation was almost exclusively cooling, whereas January 2024 was mixed-oriented, characterised by simultaneous heating and cooling within the building system, with heating dominance overall.

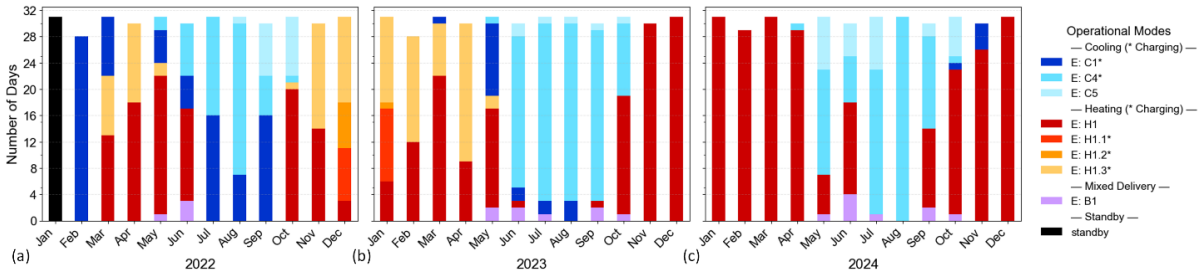


Figure 6. ECHO operating modes by month: number of days in each mode: (a) 2022, (b) 2023, (c) 2024.

4.2.2 Electricity Demand and Outdoor Temperature

Figure 7 evaluates total daily electricity consumption in varying outdoor temperatures. Electricity use remains below 0.1 MWh/day during hot summer periods, reflecting passive-cooling dominance, and rises to about 0.9–1.1 MWh/day during cold winter conditions such as January 2024. The clustering of points shows stable and repeatable behaviour under similar outdoor conditions, with no evidence of abrupt power fluctuations. The separation between cooling and heating regimes mirrors the building's operational modes, confirming predictable system response to varying weather. The wider spread visible in the 2024 cooling season is caused by a few summer days when passive cooling was limited or temporarily unavailable, forcing the heat pump to provide a larger share of the cooling demand. These mechanically dominated cooling days required substantially more electricity and therefore appear as the high-electricity outliers in the 2024 summer cluster.

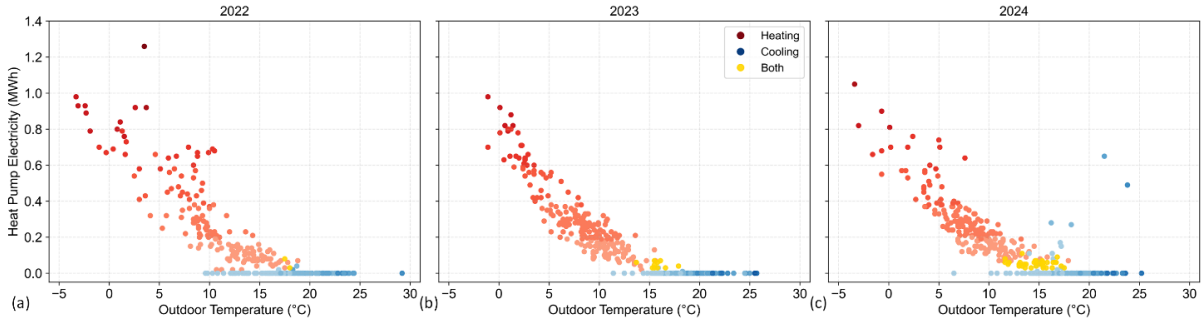


Figure 7. ECHO daily electricity consumption vs. outdoor temperature: (a) 2022, (b) 2023, (c) 2024; colour intensity indicates daily delivered thermal energy (0–7 MWh).

4.2.3 Passive Cooling and Compressor Runtime

As shown in Figure 8, cooling delivery is highest from June to September, with a peak of ≈60 MWh in June 2023. During these months, compressor runtime remains below ≈25%, and the passive-cooling share typically exceeds 80%, indicating that most cooling is provided by direct groundwater circulation with limited compressor contribution. The correlation metrics in Figure 8 further support this behaviour: compressor use shows a strong inverse correlation with delivered cold energy (F–Cold = –0.88, –0.92, –0.89 for 2022–2024), while passive-cooling share exhibits a strong positive correlation with cooling delivery (C–Cold = 0.65, 0.77, 0.89). As a result, electrical demand in the cooling season is low; when on-site PV output is high, net grid import is correspondingly reduced. In August 2024 a total of 52.6 MWh of cooling was delivered with 1.5 MWh of electricity and near-zero heat pump runtime. If the same cooling load had been produced mechanically by a chiller or heat pump with a COP of 4, electricity use would have been approximately 13.2 MWh, about 11.7 MWh (≈ 89%) higher than observed. This demonstrates the substantial reduction in electricity demand achieved through passive ATES operation and its contribution to lowering grid load during peak summer periods.

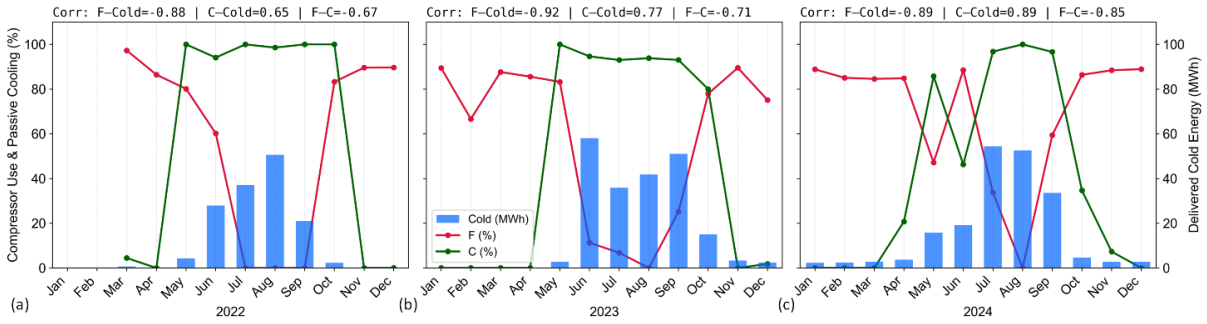


Figure 8. ECHO monthly cold energy (Cold), passive-cooling share (C), and compressor runtime fraction (F) (a–c).

During winter months, compressor runtime increases as heat pumps operate continuously for space heating. In January 2024, daily electricity use reached about 1.0 MWh, corresponding to sustained heating loads. Despite this higher electricity consumption, the system maintains heating COPs between 4 and 5 (Figure 9), consistent with efficient operation during the winter period and supported by stable aquifer temperatures (≈ 10 °C in the cold well). Overall, ECHO's ATES delivers near-passive cooling in summer and stable, efficient heating in winter.

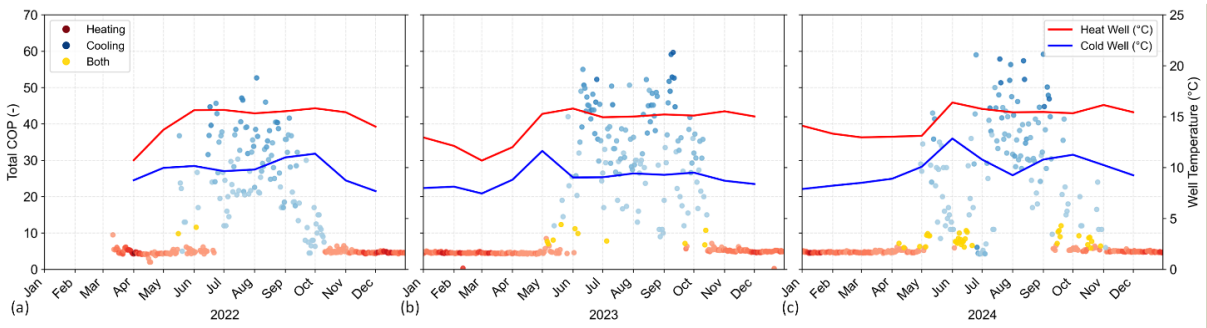


Figure 9. ECHO daily COP and well (cold or heat) temperature: (a) 2022, (b) 2023, (c) 2024.

4.2.4 Energy Balance and Regeneration Activity

As shown in Figure 10, ECHO's energy balance evolved from a cooling-dominant regime in 2022 toward improved symmetry by 2024. The large imbalance in the first observed year (≈ –80%) partly reflects the timing of system operation relative to the monitoring start date. From 2023 onward, however, the monthly imbalance stabilised and progressively narrowed to within ±15% as regeneration became more consistently applied. Regeneration was predominantly undertaken via condenser-side or dry-cooler charging during late summer. As intraday price signals and on-site PV traces were not used, summer months with high insolation and shoulder-season nights were treated as proxies for renewable-rich or off-peak conditions. The late-summer clustering of regeneration was interpreted as consistent with periods of high PV availability and, by extension, renewable-aligned operation; however, causal alignment was not established. By translating surplus (assumed available in these proxy periods) electricity into stored heat, long-term subsurface balance was enhanced and thermally self-sufficient operation within the ATES framework was supported.

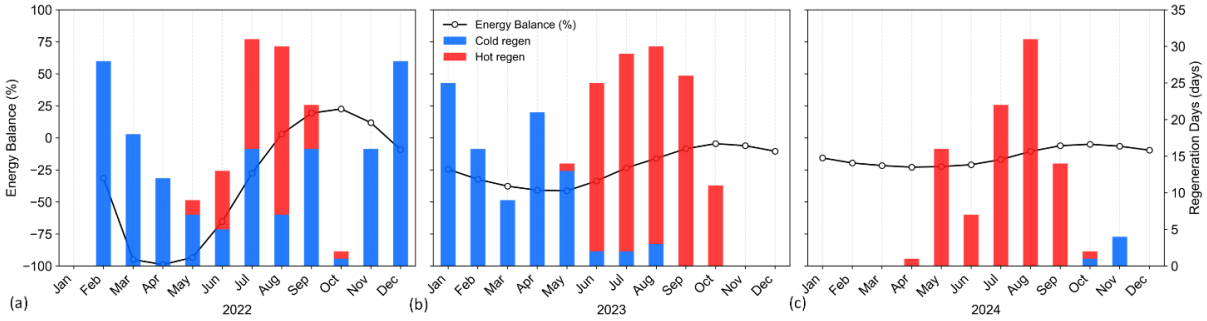


Figure 10. ECHO monthly ATES energy balance and regeneration days (a–c); regeneration includes condenser and dry-cooler charging.

5 DISCUSSION

Data resolution and mode-classification limitations should be considered when interpreting these results. As the analysis relies on daily operating-mode assignment (and monthly ATES data for ECHO), sub-daily transitions between modes are inherently aggregated. Multiple modes can occur within a single day, particularly during shoulder seasons, but only the dominant mode is captured in the daily timeline. As a result, short-duration operational switches, such as brief regeneration events, mixed heating–cooling periods, or rapid control responses, are smoothed in the aggregated data. While this approach reliably captures seasonal patterns, overall performance, and long-term balance, it may underestimate the frequency and timing of short transients. Future work could address this limitation by incorporating sub-daily (e.g., hourly) data or probabilistic disaggregation techniques to better resolve short-duration operational events and improve estimation of regeneration frequency and mode transitions.

Across both sites, ATES shifts cooling from electricity-intensive compression to passive groundwater circulation, keeping summer daily electricity use low (typically less than 0.1 MWh) and minimising coincident grid load. Passive-cooling shares are high, exceeding 80%, so most cooling requires little or no compressor input. In winter, heat pumps run continuously for space heating, but low-temperature operation (lower than 45 °C supply) and comparatively high, stable well temperatures (≈ 15 °C) sustain COP ≈ 4–5, yielding predictable, efficient electricity use rather than volatile peaks.

Seasonal regeneration underpins the durability of this electrical performance. At NEXT, coordinated (ring-based) dry-cooler and condenser-side charging maintains a near-symmetric energy balance (≈±15%) and preserves well temperatures; at ECHO, regeneration is concentrated in late summer, and the monthly balance improves toward ≈±15% by 2024. These near-balanced conditions and stable entry temperatures are consistent with sustainable ATES operation under local practice.

In E-grid terms: summer operation cuts demand and peaks via high passive shares; winter operation delivers efficient, stable electric loads (COP 4–5); and year-round, scheduling typically 5–10 regeneration days per month aligns thermal charging with low-price or renewable windows.

6 CONCLUSION

This study evaluated two operational Aquifer Thermal Energy Storage (ATES) systems at TU Delft, NEXT (ring-integrated) and ECHO (stand-alone), to quantify their contribution to grid-compatible electrified heating and cooling with a focus on electricity use.

- Summer cooling with minimal electricity: Both sites achieved high passive-cooling shares, exceeding 80%, keeping typical summer daily electricity use less than 0.1 MWh and minimising coincident grid load.
- Efficient, predictable winter heating: With low-temperature supply (≤45 °C) and stable well temperatures (≈ 15 °C), both systems maintained COP ≈ 4–5, yielding efficient, steady electric demand without volatile peaks.
- Regeneration sustains performance and balance: NEXT maintained near-symmetric seasonal energy balance (≈ ±15%) via coordinated dry-cooler and condenser-side charging, typically 5–10 days per month. ECHO moved from cooling-dominant toward balance by 2024 by aligning regeneration with PV-rich periods, effectively shifting electric use and converting surplus on-site electricity into stored heat.
- Stable electricity–temperature behaviour: Across years, both systems showed consistent clustering without abrupt fluctuations, indicating predictable, grid-friendly operation suited to planning and capacity contracting

Overall, well-controlled ATES systems reduce summer electricity needs, stabilises winter electric loads, and enables controllable thermal charging timed to renewable availability or low-price periods—acting as a flexible thermal buffer that enhances the stability and efficiency of an electrified grid.

Acknowledgements

This work is funded by INTERREG – Vlaanderen-Nederland, in the “Duurzaam Zomer Comfort” project

REFERENCES

Beernink, S., Bloemendal, M., Kleinlugtenbelt, R. & Hartog, N.: Maximizing the use of aquifer thermal energy storage systems in urban areas: effects on individual system primary energy use and overall GHG emissions, Applied Energy, 311((2022), 118587,

Bloemendal, M., Jaxa-Rozen, M. & Olsthoorn, T.: Methods for planning of ATES systems, Applied Energy, 216((2018), 534-557,

Bloemendal, M., Olsthoorn, T. & Boons, F.: How to achieve optimal and sustainable use of the subsurface for Aquifer Thermal Energy Storage, Energy policy, 66((2014), 104-114,

Buffa, S., Cozzini, M., D'antoni, M., Baratieri, M. & Fedrizzi, R.: 5th generation district heating and cooling systems: A review of existing cases in Europe, Renewable and Sustainable Energy Reviews, 104((2019), 504-522,

Buonocore, J.J., Salimifard, P., Magavi, Z. & Allen, J.G.: Inefficient building electrification will require massive buildout of renewable energy and seasonal energy storage, Scientific Reports, 12(1), (2022), 11931,

Finck, C., Li, R., Kramer, R. & Zeiler, W.: Quantifying demand flexibility of power-to-heat and thermal energy storage in the control of building heating systems, Applied Energy, 209((2018), 409-425,

Fleuchaus, P., Godschalk, B., Stober, I. & Blum, P.: Worldwide application of aquifer thermal energy storage–A review, Renewable and Sustainable Energy Reviews, 94((2018), 861-876,

Hewitt, N.J.: Electrification of Heating—Requirements for Successful Wide-Scale Deployment, Wiley Interdisciplinary Reviews: Energy and Environment, 13(6), (2024), e542,

IRENA: Thermal energy storage, Abu Dhabi, (2020).

Lee, K.S.: A review on concepts, applications, and models of aquifer thermal energy storage systems, Energies, 3(6), (2010), 1320-1334,

Li, H., Johra, H., de Andrade Pereira, F., Hong, T., Le Dréau, J., Maturo, A., Wei, M., Liu, Y., Saberi-Derakhtenjani, A. & Nagy, Z.: Data-driven key performance indicators and datasets for building energy flexibility: A review and perspectives, Applied Energy, 343((2023), 121217,

Lund, H., Werner, S., Wiltshire, R., Svendsen, S., Thorsen, J.E., Hvelplund, F. & Mathiesen, B.V.: 4th Generation District Heating (4GDH): Integrating smart thermal grids into future sustainable energy systems, energy, 68((2014), 1-11,

Nuytten, T., Claessens, B., Paredis, K., Van Bael, J. & Six, D.: Flexibility of a combined heat and power system with thermal energy storage for district heating, Applied energy, 104((2013), 583-591,